Gold Nanoparticles

DOI: 10.1002/anie.200802267

An Organometallic Approach to Gold Nanoparticles: Synthesis and X-Ray Structure of CO-Protected $Au_{21}Fe_{10}$, $Au_{22}Fe_{12}$, $Au_{28}Fe_{14}$, and $Au_{34}Fe_{14}$ Clusters**

Cristina Femoni, Maria Carmela Iapalucci, Giuliano Longoni, Cristina Tiozzo, and Stefano Zacchini*

Ligand-stabilized quasi-molecular gold nanoparticles, consisting of chunks of cubic close-packed lattice featuring "magic numbers" of gold atoms, are being intensively investigated both experimentally and theoretically,[1] owing to their potential use in miniaturized basic devices in electronics,[2] models and precursors of metallic catalysts,[3] stains of biological samples,[4] and imaging nanoprobes for drug screening and diagnosis.[5] The monodispersity of several of the above thiol/thiolate or phosphine monolayer protected gold nanoparticles has been disputed.[6] Furthermore, STM experiments and DFT calculations of adsorption of methylthiolate on Au(111) showed formation of linear RS-Au-SR staple motives.[7] This feature was later confirmed by calculations on an Au_{38} cluster of O_h symmetry,[8] and has been experimentally demonstrated by the first structural characterizations of gold–thiolate clusters, namely $[Au_{25}(SCH_2CH_2Ph)_{18}]^{-}$[9] and the giant $[Au_{102}(p\text{-MBA})_{44}]$ (p-MBA = p-mercaptobenzoic acid) cluster.[10] The only other structurally characterized gold particles exceeding 1 nm in at least one dimension are the ligand-protected $[Au_{16}(AsPh_3)_8Cl_6]$,[11] $[Au_{25}(PPh_3)_{10}(SEt)_5Cl_2]^{2+}$,[12] and $[Au_{39}(PPh_3)_{14}Cl_6]Cl_2$ clusters,[13] which do not display such a feature. Herein, we report an organometallic approach to a new kind of molecular ligand-stabilized gold nanoparticle, consisting of the synthesis of Au–Fe colloidal nanoparticles, in which $\{Fe(CO)_x\}$ ($x = 3, 4$) moieties take the place of thiol or thiolate ligands in protecting and stabilizing the gold kernel. These iron carbonyl groups share and may also exceed the bonding versatility of thiols/thiolates.[14]

The synthesis of CO-protected Au–Fe clusters involves the oxidation of $[Fe_3(CO)_{11}]^{2-}$ with $[AuCl_4]^{-}$ salts in acetone and under an inert atmosphere. After formation of the previously unknown yellow-orange $[Au_5\{Fe(CO)_4\}_4]^{3-}$ cluster, the reaction affords brown solutions of colloidal Au–Fe nanoparticles, which display broad and unresolved IR carbonyl absorptions shifting from 1960 to 2010 cm^{-1} as a function of the starting ratio of the reagents. The colloidal nature of these solutions was confirmed by dynamic light scattering (DLS) measurements in acetonitrile for two samples. The first sample (ν_{CO} at 1980 cm^{-1}) revealed the presence of two sets of nanoparticles displaying hydrodynamic diameters in the ranges 10–30 and 100–200 nm. The second sample (ν_{CO} at 1990 cm^{-1}) showed particles with nominal diameters of 35–60 and 110–300 nm. No evidence of smaller particles could be gathered. These results parallel recent measurements of solutions from which monodispersed $[Au_{25}(SCH_2CH_2Ph)_x]$ was obtained in good yields.[15]

The addition of Au^{3+} salts in excess gives rise to separation of gold powder and the formation of the dark-green $[Au\{Fe_2(CO)_8\}_2]^{-}$ cluster, two isomers of which have previously been isolated and characterized by other routes.[16] In our investigations of the above two samples we have so far isolated five molecular species, namely, $[NEt_4]_3[Au_5\{Fe(CO)_4\}_4]$ (ν_{CO} in CH_3CN at 1945s, 1861s cm^{-1}), $[NEt_4]_6[Au_{21}\{Fe(CO)_4\}_{10}]\cdot Cl$ (ν_{CO} in CH_3CN at 1982s, 1937sh, 1889sh cm^{-1}), $[NEt_4]_6[Au_{22}\{Fe(CO)_4\}_{12}]\cdot(CH_3)_2CO\cdot 0.5\,C_6H_{14}$ (ν_{CO} in CH_3CN at 1980s, 1925sh, 1880sh cm^{-1}), $[NEt_4]_8[Au_{28}\{Fe(CO)_3\}_4\{Fe(CO)_4\}_{10}]\cdot 6\,CH_3CN$ (ν_{CO} in CH_3CN at 1985s, 1927sh, 1887sh cm^{-1}) and $[NEt_4]_{10}[Au_{34}\{Fe(CO)_3\}_6\{Fe(CO)_4\}_8]\cdot 2\,Cl\cdot 7.6\,CH_3CN$ (ν_{CO} in CH_3CN at 1990s, 1932sh, 1900sh cm^{-1}). Their structures have been determined by single-crystal X-ray diffraction studies.[17]

The $[Au_5\{Fe(CO)_4\}_4]^{3-}$ cluster (**1**) is isostructural with the corresponding $[Cu_5\{Fe(CO)_4\}_4]^{3-}$[18] and $[Ag_5\{Fe(CO)_4\}_4]^{3-}$[14] species (see Figure S1 in the Supporting Information). As shown in Figure 1, $[Au_{22}\{Fe(CO)_4\}_{12}]^{6-}$ (**2**) may be formally envisioned to derive by sandwiching two $[Au_5]^{3+}$ fragments between three $[Au_4\{Fe(CO)_4\}_4]^{4-}$[19] moieties in a triple-decker fashion. The outer $\{Fe(CO)_4\}$ groups adopt C_{3v} local symmetry of the carbonyl groups and behave as triply bridging (μ_3) ligands, whereas the central $\{Fe(CO)_4\}$ groups adopt C_{2v} local symmetry of the carbonyl groups and behave as μ_4 ligands.

The $[Au_{21}\{Fe(CO)_4\}_{10}]^{5-}$ structure (**3**) may be envisioned as a molecular model of Licurgo's cup[1] (Figure 2). The metal frame consists of an inner Au-centered pentagonal antiprism, at the top and bottom of which two pentagonal Au_5Fe_5 rings are condensed. As a result the whole metal frame may be described as deriving from two fused concave cups generated by a Au_5Fe_5-Au_5-Au-Au_5-Au_5Fe_5 sequence of layers, sharing the unique Au atom and with opposite orientations. In spite of

[*] Dr. C. Femoni, Prof. M. C. Iapalucci, Prof. G. Longoni, C. Tiozzo, Dr. S. Zacchini
Dipartimento di Chimica Fisica ed Inorganica
Università di Bologna
Viale Risorgimento 4, 40136 Bologna (Italy)
Fax: (+39) 051-209-3690
E-mail: femoni@ms.fci.unibo.it

[**] Financial support from the University of Bologna (Clustercat), the MIUR (PRIN2006), and PRRIITT (Nanofaber) is gratefully acknowledged. We wish to thank Dr. Magda Blosi for her support with the DLS measurements.

Supporting information for this article is available on the WWW under http://dx.doi.org/10.1002/anie.200802267.

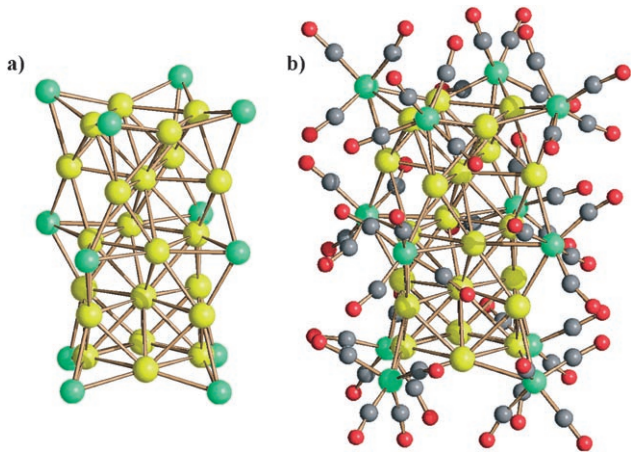

Figure 1. The metal frame (a) and the complete structure (b) of **2** (Au yellow, Fe green, C gray, O red).

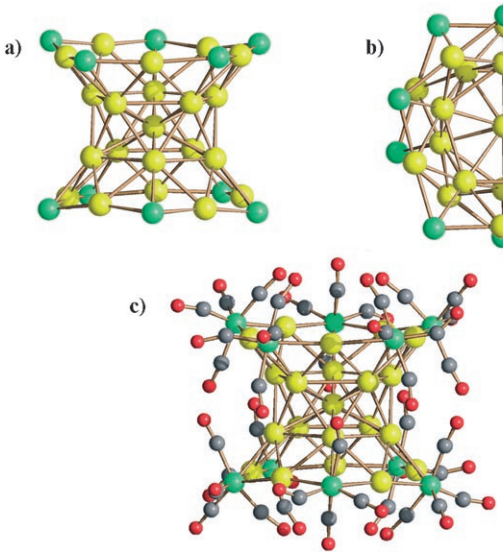

Figure 2. Two views of the metal frame (a, b) and the complete structure (c) of **3** (color legend as in Figure 1).

the width of the Au_5Fe_5 rims, the two cups do not host any molecule or ion since one CO ligand of each μ_3-$\{Fe(CO)_4\}$ fragment is directed toward the center of the rim and gives rise to a "lid" of the cup. Although such a structure does not have any precedent, certain structural motives are reminiscent of some ligand-protected Au and Au–Ag nanoparticles. Thus, the Au atoms describe two fused noncentered and incomplete icosahedrons as the bis(icosahedral) $[Ag_{12}Au_{13}(p\text{-}Tol_3P)_{10}Br_8]^+$ rotamer (Tol = tolyl).[20] Secondly, the Au_5Fe_5 rims of the two cups represent a cyclic variation of the staple motives present in both $[Au_{25}(SCH_2CH_2Ph)_{18}]^-$[9] and $[Au_{102}(p\text{-}MBA)_{44}]$.[10]

In contrast to **2** and **3**, $[Au_{28}\{Fe(CO)_3\}_4\{Fe(CO)_4\}_{10}]^{8-}$ (**4**) contains both $\{Fe(CO)_4\}$ and $\{Fe(CO)_3\}$ moieties and displays a rather complex metal frame (Figure 3 and Figure S2 in the Supporting Information). The metal framework of **4** consists of an inner tetra-capped, centered pentagonal prismatic Au_{15} core. Two fused and centered pentagonal prisms are the

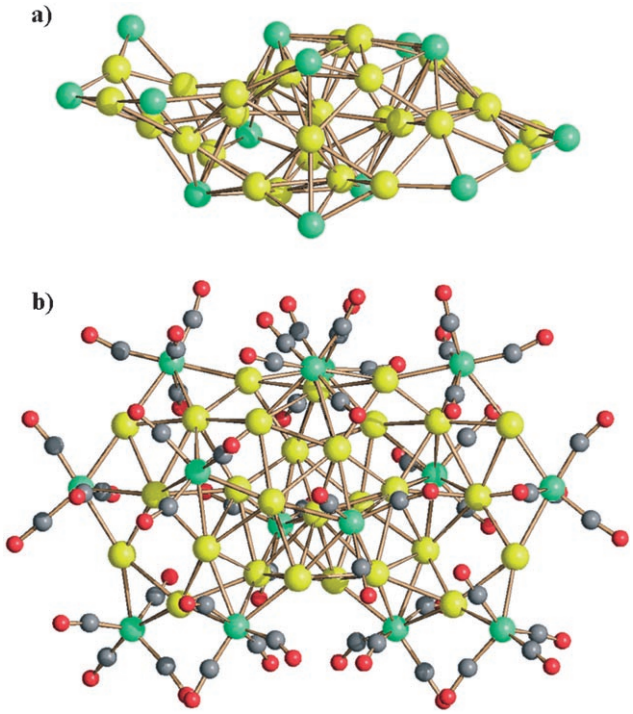

Figure 3. The metal frame (a) and the complete structure (b) of **4** (color legend as in Figure 1).

innermost core of the giant $Au_{102}(p\text{-}MBA)_{44}$ cluster.[10] Capping of the two pentagonal faces of the Au_{15} moiety with $\{Fe(CO)_3\}$ groups and addition of two $\{Au_2Fe(CO)_3\}$ moieties (to give rise to two additional $\{Au_5Fe(CO)_3\}$ pentagonal bipyramids) generates a compact $Au_{19}Fe_4$ central core of the cluster. Assembly on both sides of two quasi-planar $\{Au_5\{Fe(CO)_4\}_3\}$ and $\{Au_4\{Fe(CO)_4\}_3\}$ staples (recalling the $\{Au_3(SR)_2\}$ staples of $[Au_{25}(SCH_2CH_2Ph)_{18}]^-$[9] and $[Au_{102}(p\text{-}MBA)_{44}]$[10]) generates two dangling "baskets" with opposite orientations (up and down). The structure is then completed by capping the resulting four concave Au_4 butterfly faces with four additional μ_4-$\{Fe(CO)_4\}$ groups.

The structure of $[Au_{34}\{Fe(CO)_3\}_6\{Fe(CO)_4\}_8]^{8-}$ (**5**) is shown in Figure 4, and a step-by-step construction of the metal framework is given in Figure S3 in the Supporting Information. The Au_{34} core consists of an inner Au_6 octahedron interstitially lodged in an Au_{24} polyhedron having 6 pentagonal and 26 triangular faces (or 6 rhombic and 14 triangular faces). The above Au_{24} polyhedron is formally generated by the condensation of a pentagonal ring of gold atoms on top of each of the six vertices of the interstitial Au_6 octahedron. Capping of these six pentagonal faces with μ_6-$\{Fe(CO)_3\}$ groups gives rise to an inner $Au_{30}Fe_6$ core. Condensation of two $Au_2\{Fe(CO)_4\}_3$ staples on two opposite rhombic faces of the $Au_{30}Fe_6$ core generates two outer distorted trigonal prisms with an edge bridged by a μ-$\{Fe(CO)_4\}$ group and the two triangular faces capped by μ_4-$\{Fe(CO)_4\}$ groups. Finally, two μ_3-$\{Fe(CO)_4\}$ groups cap two opposite rhombic faces and complete the shielding of the gold particle. Once again, a staple motif is present as for $[Au_{25}(SCH_2CH_2Ph)_{18}]^-$,[9] $[Au_{102}(p\text{-}MBA)_{44}]$,[10] **3**, and **4**.

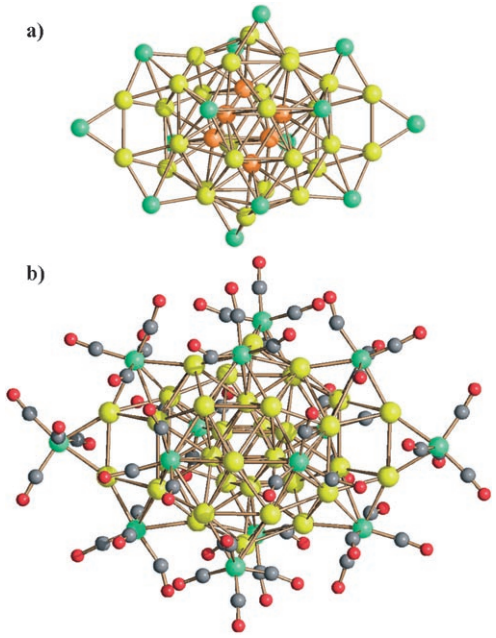

Figure 4. The metal frame (a) and the complete structure (b) of **5** (color legend as in Figure 1; the interstitial Au_6 octahedral moiety in (a) is marked in orange).

In conclusion, framework fragments of C_5 local symmetry seem to dominate all structures, with the notable exception of **2**. Even relatively small variations in composition of otherwise similarly sized CO-protected Au–Fe clusters result in large changes of the structure of the gold kernel. These changes are probably favored by the bonding versatility of the $\{Fe(CO)_4\}$ and $\{Fe(CO)_3\}$ moieties. However, the correspondence of some structural motives between the so far structurally characterized thiolate-protected gold clusters and the title compounds confirms the need of some wariness in determining supposedly molecular features by measurements carried out on collections of quasi-monodispersed ligand-protected gold nanoparticles, rather than a single nanoparticle.[21]

Moreover, staple motives, the oxidation state of surface gold atoms, and the energy of Au atomic orbitals are likely to concur in delaying the insulator-to-metal transition as their nuclearity increases, relative to the more compact transition-metal carbonyl clusters.[22] As suggested by EHMO calculations, the HOMO–LUMO gaps of **2–5** are in the range 0.8–1.3 eV (see the Supporting Information), in fair agreement with calculated[8] and experimental values of monodispersed Au_{38} molecule-like nanoparticles.[23]

The measured diameters of CO-protected Au–Fe nanoparticles deserve some specific comments. Indeed, as shown in Table 1, these are at least one and two orders of magnitude smaller than those suggested by DLS experiments. A plausible explanation is that the above highly charged cluster anions are present in solution as cation–anion aggregates. Partially in keeping with this suggestion, the hydrodynamic diameters determined for the same sample in acetonitrile and DMSO are different. In the latter, there is clear evidence of nanoparticles of approximately 4 nm, in addition to other spread in the ranges 8–40 and 100–300 nm. The lowest value is in line with the dimensions of **2–5** within the first coordination sphere of the solvent cage.

Table 1: Maximum diameters (nm) of the metal frames.[a]

	2	3	4	5
A	1.53	1.353	1.85	1.92
B	2.14	1.90	2.40	2.43

[a] Measured (X-ray structure) from the outermost Fe nuclei including twice the Fe metal radius (A), and the outermost oxygen atoms including twice the van der Waals radius of oxygen (B).

It is, however, possible that some decomposition under laser radiation could also contribute to the large diameters detected. Finally, it can be anticipated that the above CO-protected Au–Fe clusters may turn out to be valuable precursors of miscellaneous inorganic oxide–metal composites of potential interest in the rapidly expanding field of gold catalysis.[3] Thermal treatment of their $[NEt_4]^+$ salts gives rise to Au, Au–Fe, or $Au_nFe_xO_y$ powders, as a function of experimental conditions. The study of their catalytic performances is underway.[24]

Experimental Section

A solution of $[NEt_4][AuCl_4]$ (0.60 g, 0.62 mmol) in acetone (10 mL) was slowly added to a solution of $[NEt_4]_2[Fe_3(CO)_{11}]$ (0.36 g, 0.62 mmol) in acetone (30 mL) under N_2. The final molar ratio was finely adjusted with small additions of $[NEt_4][AuCl_4]$ to tune the main carbonyl absorption to 1980 cm^{-1}. The resulting dark brown suspension was filtered, and the filtrate was dried in vacuum and washed with THF (3×10 mL) to eliminate $[NEt_4][AuFe_4(CO)_{16}]$. A first extraction with acetone (20 mL) and precipitation by layering *n*-hexane gave orange crystals of $[NEt_4]_3[Au_5Fe_4(CO)_{16}]$ (minor product) and black crystals of $[NEt_4]_6[Au_{22}Fe_{12}(CO)_{48}]\cdot(CH_3)_2CO\cdot0.5C_6H_{14}$ (yield 20% based on Au. Anal. results (%) found: Au 59.6, Fe 9.51; calcd: Au 59.94, Fe 9.29). Subsequent extraction of the residue with acetonitrile (20 mL) and precipitation by layering diisopropyl ether gave black crystals of $[NEt_4]_6[Au_{21}Fe_{10}(CO)_{40}]\cdot Cl$ (yield 5% based on Au. Elemental analysis (%): found: Au 62.1, Fe 8.32; calcd: Au 62.38, Fe 8.44).

The same procedure was applied for the synthesis of the second sample, the only variation being a fine tuning of the main IR carbonyl absorption to 1990 cm^{-1}. The resulting dark brown suspension was filtered, and the filtrate was dried in vacuum and washed with THF (3×10 mL) to eliminate $[NEt_4][AuFe_4(CO)_{16}]$ and with acetone (2×10 mL) to eliminate $[NEt_4]_3[Au_5Fe_4(CO)_{16}]$ and $[NEt_4]_6[Au_{22}Fe_{12}(CO)_{48}]$. A first extraction of the residue with acetonitrile (10 mL) and precipitation by layering diisopropyl ether gave black crystals of $[NEt_4]_8[Au_{28}Fe_{14}(CO)_{52}]\cdot6CH_3CN$ (yield 15% based on Au. Anal. results (%) found: Au 61.3, Fe 8.42; calcd: Au 61.00, Fe 8.67). A second extraction with acetonitrile (20 mL) gave black crystals of $[NEt_4]_{10}[Au_{34}Fe_{14}(CO)_{50}]\cdot2Cl\cdot7.6CH_3CN$ (yield 20% based on Au. Elemental analysis (%): found: Au 63.20, Fe 7.50; calcd: Au 63.31, Fe 7.41) The overall yield of Au–Fe carbonyl species (including the yet uncharacterized ones) measured by Au analysis of the filtered reaction solutions was greater than 70%.

Received: May 15, 2008
Published online: July 23, 2008

Keywords: cluster compounds · gold · iron · nanoparticles

[1] M.-C. Daniel, D. Astruc, *Chem. Rev.* **2004**, *104*, 293 – 346.
[2] G. Schmid, U. Simon, *Chem. Commun.* **2005**, 697 – 710.
[3] A. S. K. Hashmi, G. J. Hutchings, *Angew. Chem.* **2006**, *118*, 8064 – 8105; *Angew. Chem. Int. Ed.* **2006**, *45*, 7896 – 7936.
[4] P. Schwerdtfeger, *Angew. Chem.* **2003**, *115*, 1936 – 1939; *Angew. Chem. Int. Ed.* **2003**, *42*, 1892 – 1895.
[5] S. Lee, E.-J. Cha, K. Park, S.-Y. Lee, J.-K. Hong, I.-C. Sun, S. Y. Kim, K. Choi, I. C. Kwon, K. Kim, C.-H. Ahn, *Angew. Chem.* **2008**, *120*, 2846 – 2849; *Angew. Chem. Int. Ed.* **2008**, *47*, 2804 – 2807.
[6] D. H. Rapoport, W. Vogel, H. Cölfen, R. Schlögl, *J. Phys. Chem. B* **1997**, *101*, 4175 – 4183.
[7] P. Maksymovic, D. C. Sorescu, J. T. Yates, *Phys. Rev. Lett.* **2006**, *97*, 146103.
[8] D. Jiang, M. L. Tiago, W. Luo, S. Dai, *J. Am. Chem. Soc.* **2008**, *130*, 2777 – 2779.
[9] M. W. Heaven, A. Dass, P. S. White, K. M. Holt, R. W. Murray, *J. Am. Chem. Soc.* **2008**, *130*, 3754 – 3755.
[10] P. D. Jadzinsky, G. Calero, C. J. Ackerson, D. A. Bushnell, R. D. Kornberg, *Science* **2007**, *318*, 430 – 433.
[11] M. Richter, J. Strähle, *Z. Anorg. Allg. Chem.* **2001**, *627*, 918 – 920.
[12] Y. Shichibu, Y. Negishi, T. Watanabe, N. K. Chaki, H. Kawaguchi, T. Tsukuda, *J. Phys. Chem. C* **2007**, *111*, 7845 – 7847.
[13] B. K. Teo, X. Shi, H. Zhang, *J. Am. Chem. Soc.* **1992**, *114*, 2743 – 2745.
[14] V. G. Albano, F. Azzaroni, M. C. Iapalucci, G. Longoni, M. Monari, S. Mulley, D. M. Proserpio, A. Sironi, *Inorg. Chem.* **1994**, *33*, 5320 – 5328.
[15] M. Zhou, E. Lanni, N. Garg, M. E. Bier, R. Jin, *J. Am. Chem. Soc.* **2008**, *130*, 1138 – 1139.
[16] V. G. Albano, M. Monari, F. Demartin, P. Macchi, C. Femoni, M. C. Iapalucci, G. Longoni, *Solid State Sci.* **1999**, *1*, 597 – 606.
[17] Crystal data for: $[NEt_4]_3$-**1:** $M_r = 2047.14$, $0.18 \times 0.15 \times 0.11$ mm^3, tetragonal, $P4(2)/mmm$, $a = 13.9843(6)$, $c = 14.2247(13)$ Å, $V = 2781.8(3)$ Å^3, $Z = 2$, $\rho = 2.444$ g cm^{-3}, $\mu = 14.202$ mm^{-1}, $Mo_{K\alpha}$ radiation ($\lambda = 0.71073$ Å), $T = 293$ K, $2.04 < \theta < 26.99$, 29958 collected and 1671 independent reflections, ($R_{int} = 0.0984$), $R_1 = 0.0442$ [$I > 2\sigma(I)$], $wR_2 = 0.1385$. Crystal data for $[NEt_4]_6$-**2**·$(CH_3)_2CO$·0.5 C_6H_{14}: $M_r = 7230.61$, $0.10 \times 0.08 \times 0.07$ mm^3, orthorhombic, $Pbca$, $a = 24.676(2)$, $b = 25.121(2)$, $c = 47.157(4$ Å, $V = 29232(5)$ Å^3, $Z = 8$, $\rho = 3.286$ g cm^{-3}, $\mu = 23.204$ mm^{-1}, $Mo_{K\alpha}$, radiation ($\lambda = 0.71073$ Å), $T = 100$ K, $1.44 < \theta < 25.00$, 203390 collected and 25725 independent reflections, ($R_{int} = 0.3886$), $R_1 = 0.0719$ [$I > 2\sigma(I)$], $wR_2 = 0.22325$. $[NEt_4]_6$-**3**·Cl: $M_r = 6632.15$, $0.10 \times 0.08 \times 0.07$ mm^3, monoclinic, $C2/c$, $a = 31.137(8)$, $b = 17.112(5)$, $c = 27.511(8)$ Å, $\beta = 112.372(3)°$, $V = 13555(6)$ Å^3, $Z = 4$, $\rho = 3.250$ g cm^{-3}, $\mu = 23.742$ mm^{-1}, $Mo_{K\alpha}$ radiation ($\lambda = 0.71073$ Å), $T = 298$ K, $1.38 < \theta < 25.00$, 63907 collected and 11945 independent reflections, ($R_{int} = 0.2796$), $R_1 = 0.0861$ [$I > 2\sigma(I)$], $wR_2 = 0.3347$. $[NEt_4]_8$-**4**·6CH_3CN: $M_r = 9041.81$, $0.09 \times 0.08 \times 0.07$ mm^3, triclinic, $P\bar{1}$, $a = 19.2707(13)$, $b = 20.2954(14)$, $c = 26.0761(17$ Å, $\alpha = 86.7930(10)$, $\beta = 89.2540(10)$, $\gamma = 63.4330(10)°$, $V = 9106.6(11)$ Å^3, $Z = 2$, $\rho = 3.297$ g cm^{-3}, $\mu = 23.596$ mm^{-1}, $Mo_{K\alpha}$ radiation ($\lambda = 0.71073$ Å), $T = 100$ K, $1.21 < \theta < 25.00$, 87885 collected and 31967 independent reflections, ($R_{int} = 0.1494$), $R_1 = 0.0622$ [$I > 2\sigma(I)$], $wR_2 = 0.1455$. $[NEt_4]_{10}$-**5**·2 Cl·7.6 CH_3CN: $M_r = 10564.67$, $0.10 \times 0.09 \times 0.08$ mm^3, monoclinic, $C2/c$, $a = 38.126(10)$, $b = 28.638(8)$, $c = 21.105(6$ Å, $\beta = 105.800(3)°$, $V = 22172(10)$ Å^3, $Z = 4$, $\rho = 3.165$ g cm^{-3}, $\mu = 23.362$ mm^{-1}, $Mo_{K\alpha}$ radiation ($\lambda = 0.71073$ Å), $T = 100$ K, $1.42 < \theta < 25.00$, 101964 collected and 19541 independent reflections, ($R_{int} = 0.2797$), $R_1 = 0.0829$ [$I > 2\sigma(I)$], $wR_2 = 0.2733$. CCDC 687788 (**1**), 687789 (**3**), 687790 (**2**), 687791 (**4**), and 687792 (**5**) contain the supplementary crystallographic data for this paper. These data can be obtained free of charge from The Cambridge Crystallographic Data Centre via www.ccdc.cam.ac.uk/data_request/cif.
[18] G. Doyle, K. A. Eriksen, D. Van Engen, *J. Am. Chem. Soc.* **1986**, *108*, 445 – 451.
[19] V. G. Albano, F. Calderoni, M. C. Iapalucci, G. Longoni, M. Monari, *J. Chem. Soc. Chem. Commun.* **1995**, 433 – 434.
[20] B. K. Teo, H. Zhang, *Angew. Chem.* **1992**, *104*, 447 – 449; *Angew. Chem. Int. Ed. Engl.* **1992**, *31*, 445 – 447.
[21] R. L. Whetten, R. C. Price, *Science* **2007**, *318*, 407 – 408.
[22] C. Femoni, M. C. Iapalucci, F. Kaswalder, G. Longoni, S. Zacchini, *Coord. Chem. Rev.* **2006**, *250*, 1580 – 1604.
[23] D. Lee, R. L. Donkers, G. Wang, A. S. Harper, R. W. Murray *J. Am. Chem. Soc.* **2004**, *126*, 6193 – 6199.
[24] S. Albonetti, R. Bonelli, J. E. Mengou, C. Femoni, C. Tiozzo, S. Zacchini, F. Trifirò, *Catal. Today* **2008**, DOI: 10.1016/j.cattod.2007.11.003.

